An automated approach for updating land cover maps based on integrated change detection and classification methods

Article *in* ISPRS Journal of Photogrammetry and Remote Sensing · June 2012

DOI: 10.1016/j.isprsjprs.2012.05.006

CITATIONS
96

READS
717

4 authors, including:

Xuehong Chen
Beijing Normal University
72 PUBLICATIONS **1,532** CITATIONS

SEE PROFILE

Jin Chen
Beijing Normal University
204 PUBLICATIONS **6,807** CITATIONS

SEE PROFILE

Yasushi Yamaguchi
Nagoya University
207 PUBLICATIONS **5,027** CITATIONS

SEE PROFILE

ISPRS Journal of Photogrammetry and Remote Sensing 71 (2012) 86–95

Contents lists available at SciVerse ScienceDirect

ISPRS Journal of Photogrammetry and Remote Sensing

journal homepage: www.elsevier.com/locate/isprsjprs

An automated approach for updating land cover maps based on integrated change detection and classification methods

Xuehong Chen [a,b], Jin Chen [b,*], Yusheng Shi [a], Yasushi Yamaguchi [a]

[a] Graduate School of Environmental Studies, Nagoya University, Nagoya 464-8601, Japan
[b] State Key Laboratory of Earth Surface Processes and Resource Ecology, Beijing Normal University, Beijing 100875, China

ARTICLE INFO

Article history:
Received 14 November 2011
Received in revised form 22 March 2012
Accepted 10 May 2012

Keywords:
Land cover
Change detection
Classification
Iterated training sample selecting
Markov random fields

ABSTRACT

Updating land cover maps from remotely sensed data in a timely manner is important for many areas of scientific research. Unfortunately, traditional classification procedures are very labor intensive and subjective because of the required human interaction. Based on the strategy of updating land cover data only for the changed area, we proposed an integrated, automated approach to update land cover maps without human interaction. The proposed method consists primarily of the following three parts: a change detection technique, a Markov Random Fields (MRFs) model, and an iterated training sample selecting procedure. In the proposed approach, remotely sensed data acquired in different seasons or from different remote sensors can be used. Meanwhile, the approach is completely unsupervised. Therefore, the methodology has a wide scope of application. A case study of Landsat data was conducted to test the performance of this method. The experimental results show that several sub-modules in this method work effectively and that reasonable classification accuracy can be achieved.

1. Introduction

Information regarding land cover composition and changes is valuable for studying multiple aspects of an environmental system, such as energy balance, biogeochemical cycles, hydrological cycles and the climate system, which are regarded as crucial elements in global change studies (Turner et al., 1995). Therefore, reliable land cover information from remotely sensed data is increasingly required at a continuum of scales, from local and regional to continental and global scales. At global scales, several land cover datasets derived from remotely sensed data are available currently, including IGBP DISCover (Loveland et al., 2000), the MODIS land cover product (Friedl et al., 2002), the UMD land cover product (Hansen et al., 2000), and global land cover 2000 (Bartholomé and Belward, 2005). All of the above datasets are at a spatial resolution of 1 km. Additionally, another global land cover dataset, GlobCover produced by European Space Agency (ESA), is at a resolution of 300 m (Arino et al., 2008). However, previous studies have shown that there is relatively little agreement between these global land cover datasets (Hansen and Reed, 2000; Iwao et al., 2006; Kaptué Tchuenté et al., 2011), which could decrease the reliability of the related studies. Additionally, these coarse resolution land cover products cannot satisfy the requirements of some specific studies, such as landscape analysis and land resources management at regional scales. Another important issue that has been found in the existing land cover products is that these products are derived only from remotely sensed data acquired during one or several years and represent land cover characteristics for a specific period with a lack of long-term land cover change information. At a regional scale, most land cover/use maps were derived from medium spatial resolution data, such as Landsat, Advanced Space-borne Thermal Emission and Reflection Radiometer (ASTER), and SPOT High-Resolution Visible and Infrared (HRVIR). Although the potential exists to achieve better classification accuracy, much human intervention is required in the classification procedure that cannot satisfy the requirement for the timely extraction of land cover information based on the large and growing satellite data archives of the Earth's surface.

Although many computer-aided techniques have been developed for land cover classification or change detection during the past decades (Canty, 2006; Lu and Weng, 2007; Lu et al., 2004), the skills and experience of an analyst are still very important for the success of image classification (Weng, 2011; Aitkenhead and Aalders, 2011) because the required human intervention is labor consuming and subjective. Moreover, the lack of historical and coincidental ground information to either establish training data or assess identification accuracy also decreases the accuracy of land cover maps and the flexibility of classification and change detection algorithms (Xie et al., 2010). Therefore, the reliable classification of large amounts of remotely sensed data remains a very challenging task (Franklin and Wulder, 2002).

* Corresponding author. Tel.: +86 13522889711.
E-mail address: chenjin@bnu.edu.cn (J. Chen).

0924-2716/$ - see front matter © 2012 International Society for Photogrammetry and Remote Sensing, Inc. (ISPRS) Published by Elsevier B.V. All rights reserved.
http://dx.doi.org/10.1016/j.isprsjprs.2012.05.006

A promising solution to the aforementioned technical difficulties in land cover map updating is to best utilize a known classification map instead of independently classifying the remotely sensed images. Xian et al. (2009) proposed a technique to update the 2001 national land cover database using a change detection method. In that study, Change Vector Analysis (CVA) was first employed to detect changed areas and then the detected changed areas were reclassified using Decision Tree Classification (DTC). This technique is capable of producing a reasonably accurate land cover map in a cost-effective way. However, CVA has a strict requirement for remotely sensed data that two used images acquired in different years should come from the same phenological period (Chen et al., 2003), which limits its wide application. In many cases, multi-seasonal data are strongly recommended because these data are not only useful for classifying different vegetation types (Saadat et al., 2011; Maxwell et al., 2004) but also for correctly identifying land cover that changes seasonally, such as water bodies and snow cover (Ho and Umitsu, 2011; Negi et al., 2009). Unfortunately, acquiring such data in similar multi-seasons for both of the two years is very difficult because of cloud contamination. Furthermore, a single CVA threshold is not appropriate for detecting the area of different change types (Xian et al., 2009), which increases the difficulty of determining a suitable threshold. Another approach, the Tempo-Spatial Feature Evolution (T-SFE) model (Xie et al., 2010), was proposed to address the difficulty of acquiring a historical training dataset for the classification of remotely sensed data. This model first produces the spectral class map by the unsupervised ISODATA classifier and then assigns the spectral class to the ground cover type by referring to a reference map of ground cover types from a subsequent time. Although this method avoids the requirement for a classification training dataset, the T-SFE model is only an exploratory rather than an automatic method because a satisfactory classification result requires the proper calibration of various model parameters.

Although CVA–DTC has limitations, the strategy of updating land cover data only for the changed areas is promising. Therefore, we developed a new approach to update land cover maps by improving the updating strategy of Xian. The proposed approach aims to achieve two objectives: (1) to reduce the CVA requirement for remotely sensed imageries that should be acquired in the same phenological period from different years; and (2) to generate a fully unsupervised, automated method without human interaction for training data collection and parameter calibration. In the proposed approach, the Maximum Likelihood Classifier (MLC), which is the most popular supervised classification method in application studies, is employed for classification. The straightforward change detection technique, Change Vector Analysis in Posterior Probability Space (CVAPS) (Chen et al., 2011) or Post Classification Comparison (PCC), are employed for change detection. Compared with CVA, PCC and CVAPS have relatively low requirements for remotely sensed data. Data acquired in different seasons or even with different remote sensors can be used (Serra et al., 2003). Considering the cumulative error in PCC (Macleod and Congalton, 1998; Castellana et al., 2007; Chen et al., 2011), CVAPS is recommended here because it can inherit the advantages of CVA and PCC. The greatest challenge in our method is to properly select the training sample. We proposed an iterated procedure to select training samples automatically based on a known classification map to ensure that the method is completely unsupervised. Additionally, an approach based on the Markov Random Fields (MRFs) model was employed to reduce the "salt-and-pepper" error that usually occurs in pixel-based classification methods. A case study using Landsat data was conducted to validate the effectiveness of the proposed method, and the new method is expected to be more practicable for land cover updating or historical land cover mapping than CVA–DTC in common application cases with an available land cover map for a certain year.

2. Methodology

The proposed approach consists of three main parts: the change detection method, the Markov Random Fields (MRFs) model, and an iterated training sample selecting procedure. The general flowchart is shown in Fig. 1.

2.1. Change detection method

The change detection methods can be categorized into two types: (1) methods based on the radiometric difference between different acquisition dates, such as CVA; and (2) methods based on the classification results of the satellite images, such as PCC and CVAPS. The former method requires the used data should be acquired in the same phenological period and from the same remote sensors. In contrast, the latter methods do not have such strict requirement, therefore were selected in this study. PCC detects the changed areas by directly comparing two classification maps. This method is straightforward and easily conducted but suffers from cumulative error, which means that the change detection result will be incorrect if classification error happens in any one of the two images from different years (Chen et al., 2003, 2011; Liu et al., 2006; Castellana et al., 2007). As the classification error usually happens in the mixed pixels, PCC will make many unchanged mixed pixels as changed pixels even though the spectra change slightly (Chen et al., 2011).

As an improvement, CVAPS compares the posterior probability maps for two different dates instead of the classified maps, which

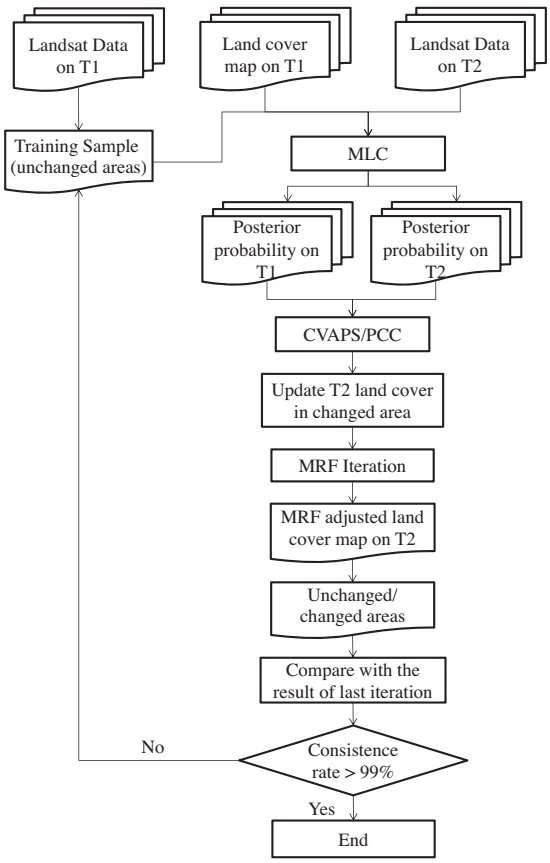

Fig. 1. Flowchart of the proposed approach.

avoids cumulative error (Chen et al., 2011). Supervised classifiers can be used to estimate the posterior probabilities of different land cover types. Here, a standard Maximum Likelihood Classifier (MLC) was used for its high computing efficiency and acceptable accuracy. In MLC, the normal distribution model is adopted. Assuming that the posterior probability vectors of a pixel at Times 1 and 2 are $\mathbf{P}^{(1)}$ and $\mathbf{P}^{(2)}$, respectively, the change vector in a posterior probability space can be defined as

$$\Delta\mathbf{P} = \mathbf{P}^{(2)} - \mathbf{P}^{(1)} = \begin{pmatrix} p_1^{(2)} \\ p_2^{(2)} \\ \dots \\ p_m^{(2)} \end{pmatrix} - \begin{pmatrix} p_1^{(1)} \\ p_2^{(1)} \\ \dots \\ p_m^{(1)} \end{pmatrix}, \quad (1)$$

where m is the number of classes. $\Delta\mathbf{P}$ represents the difference in the posterior probability of each class for the two dates and contains the change information between the two images. The change magnitude of the vector is calculated as

$$\|\Delta\mathbf{P}\| = \sqrt{\sum_{i=1}^{m} (p_i^{(2)} - p_i^{(1)})^2}. \quad (2)$$

Compared with CVA, $\|\Delta\mathbf{P}\|$ of different change types are at the same scale because the posterior probability can normalize the intra-class variability and inter-class distance. When the $\|\Delta\mathbf{P}\|$ value is greater, the probability of change is higher. Compared with PCC, CVAPS requires a threshold to determine the changed/unchanged pixels. The threshold can be determined by either a supervised or unsupervised method. Here, the unsupervised threshold determination method based on the histogram entropy (Kapur et al., 1985) was employed to ensure that the method was unsupervised, although the supervised method is capable of achieving higher change detection accuracy (Chen et al., 2011).

Although some non-parametric classification algorithms, such as Support Vector Machine (SVM) and Artificial Neural Net (ANN), have been found to perform better than MLC in some studies (e.g., Dixon and Candade, 2007; Mountrakis et al., 2011), these algorithms were not considered in this study because their computation cost increases geometrically with the increase in training sample size.

2.2. Markov random fields model

Pixel-based change detection (or classification) methods usually generate more "salt-and-pepper" error (Lu and Weng, 2007). One solution is to employ an object-based classification method, which has recently received increasing attention (Blaschke, 2010). However, such methods require many parameters, which are usually difficult to determine and do not satisfy the requirements of our automated method. Another solution is post-classification processing, such as the majority filter and the MRF model. In the past decades, the MRF model has been introduced in many change detection studies and has been shown to be effective at reducing "salt-and-pepper" error (e.g., Jeon and Landgrebe, 1991; Solberg et al., 1996; Bruzzone and Prieto, 2000; Liu et al., 2008). Compared to the object based classification method, the MRF model requires fewer parameters and has greater computing efficiency because parallel computing and advanced optimization algorithms are available for the MRF model (Sui et al., 2012; Szeliski et al., 2008). Therefore, the MRF model introduced in Bruzzone and Prieto (2000) was employed to reduce the "salt-and-pepper" error. In the MRF model, the probability of the pixel (i,j) belonging to the class C_l is determined by both the spectral information and the labels of the neighboring pixels:

$$P(C_l(i,j)) = \frac{1}{Z}\exp\left\{-\left(U_{\text{context}}[C_l(i,j)] + U_{\text{spectrum}}[C_l(i,j)]\right)\right\}, \quad (3)$$

where Z is the normalizing constant; U_{context} and U_{spectral} is the energy of the context and the spectrum, respectively. The energy of the spectrum is the log function of the posterior probability:

$$U_{\text{spectrum}}[C_l(i,j)] = -\ln(p_{\text{spectrum}}[C_l(i,j)]), \quad (4)$$

where p_{spectral} is the posterior probability that is derived from the MLC classifier. The energy of the context is calculated based on the labels of the neighboring pixels. For the target pixel (i,j), a set of neighbor pixels called $\mathbf{N}(i,j)$, is defined first. As is the case in previous studies, a second-order neighborhood set (Fig. 2) is employed:

$$\mathbf{N}(i,j) = \{(i\pm1,j),(i,j\pm1),(i+1,j\pm1),(i-1,j\pm1)\}. \quad (5)$$

Then the energy of the context is calculated as follows:

$$\begin{aligned} U_{\text{context}}[C_l(i,j)] &= U_{\text{context}}\left(\frac{C_l(i,j)}{\{C_l(g,h),(g,h)\in\mathbf{N}(i,j)\}}\right) \\ &= \sum \beta\delta_k(C_l(i,j),C_l(g,h)), \end{aligned} \quad (6)$$

where

$$\delta_k(C_l(i,j),C_l(g,h)) = \begin{cases} -1, & \text{if } C_l(i,j) = C_l(g,h) \\ 0, & \text{if } C_l(i,j) \neq C_l(g,h) \end{cases}, \quad (7)$$

and β is the weight coefficient of the context information. Here, this value was set as 1.6 based on the study of Bruzzone and Prieto (2000). The MRF model determines the class by minimizing the energy function (equivalent to maximizing the probability function) in Eq. (3) using the optimization algorithm such as iterated conditional modes (ICM), metropolis, graph cuts, and loopy belief propagation (LBP) (Besag, 1986; Kohli and Torr, 2007; Szeliski et al., 2008). In this paper, the traditional ICM algorithm was employed for its acceptable efficiency and accuracy in the classification of remotely sensed images (Bruzzone and Prieto, 2000; Liu et al., 2008). It is noticed that only the changed pixels detected in Section 2.1 were refined by MRF model. The iteration of ICM can be described as follows:

1. For all changed pixels determined by the pixel-based change detection technique, initialize $C_l(i,j)$ with the class that minimizes the spectral energy function. The initialized classification is equal to the MLC result.
2. For all changed pixels, update $C_l(i,j)$ to the class that minimizes the total energy function (Eq. (3)).
3. Repeat Step 2 until convergence is reached.

After iteration, the isolated changed pixels are more likely to be marked as unchanged pixels; therefore, the "salt-and-pepper" error can be reduced.

2.3. Training sample selection

The key step of the automated approach is the proper selection of the training samples because they are required for MLC, PCC and CVAPS. Traditionally, the training samples are selected manually depending on the knowledge of the analyst or field investigation, which is time-consuming and subjective. It is assumed that the re-

(i-1, j-1)	(i, j-1)	(i+1, j-1)
(i-1, j)	(i, j)	(i+1, j-1)
(i-1, j+1)	(i, j+1)	(i+1, j+1)

Fig. 2. Second-order neighborhood set used by the MRF model.

motely sensed images were acquired in the year of T1 and T2 respectively and a classification map is already available on T1. The training sample for T2 is selected based on the known classification map on T1. Usually, the land cover changes only occurred in small areas between T1 and T2 for most applications, consequently, the use of the unchanged areas as training samples for the image on T2 is reasonable. Therefore, we developed an iterated method to refine the unchanged area as training samples. For convenience of description, the image data on T1 and T2 are denoted as $\mathbf{\Psi}_1$ and $\mathbf{\Psi}_2$, and the classification maps on T1 and T2 are denoted as $\mathbf{C}_1$ and $\mathbf{C}_2$. The training sample set is denoted as $\mathbf{\Omega}$. The iteration procedure includes following steps:

1. All of the pixels in the known classification map on T1 are first selected into training samples set: $\mathbf{\Omega} = \mathbf{C}_1$.
2. The $\mathbf{\Omega}$ is used for training the MLC for the calculation of posterior probability vectors on T1 and T2.
3. Changed/unchanged areas are detected by a pixel-based change detection method (CVAPS or PCC). The sets of changed pixels and unchanged pixel are denoted as $\mathbf{\Theta}_c$ and $\mathbf{\Theta}_u$.
4. The T2 land cover types of the changed pixels $\mathbf{C}_2(\mathbf{\Theta}_c)$ are updated according to the MLC results, and unchanged pixels $\mathbf{C}_2(\mathbf{\Theta}_u)$ inherit the land cover labels from the T1 land cover map.

$$\begin{cases} \mathbf{C}_2(\mathbf{\Theta}_c) = \mathrm{MLC}(\mathbf{\Omega}, \mathbf{\Psi}_2, \mathbf{\Theta}_c) \\ \mathbf{C}_2(\mathbf{\Theta}_u) = \mathbf{C}_1(\mathbf{\Theta}_u) \end{cases} \tag{8}$$

5. The T2 land cover map $\mathbf{C}_2 = \{\mathbf{C}_2(\mathbf{\Theta}_c), \mathbf{C}_2(\mathbf{\Theta}_u)\}$ is refined using the MRF model.

$$\mathbf{C}_{2M} = \mathrm{MRF}(\mathbf{C}_2), \tag{9}$$

and a more aggregate changed/unchanged map is obtained by comparing $\mathbf{C}_{2M}$ and $\mathbf{C}_1$. The sets of unchanged pixels and changed pixels are refined as $\mathbf{\Theta}_{uM}$ and $\mathbf{\Theta}_{cM}$

6. The unchanged pixels are re-selected as training samples $\mathbf{\Omega} = \mathbf{C}_1(\mathbf{\Theta}_{uM})$ and goto step (2).

The Steps (2)–(6) is repeated until the $\mathbf{\Theta}_{uM}$ and $\mathbf{\Theta}_{cM}$ are highly consistent with the result of last iteration at the rate of 99%. The consistence rate is defined as:

$$\text{Consistence rate} = \frac{p_{\text{unchanged}} + p_{\text{changed}}}{P}, \tag{10}$$

where p_{changed} is the number of pixels that are marked as unchanged pixels in both iterations, and p_{changed} is the number of pixels that are marked as changed pixels in both iterations. P is the number of all of the pixels in the image. Consequently, a higher consistency rate indicates that a change in the training samples has less influence on the changed/unchanged pixel detection result. This iterated procedure is expected to refine the unchanged area as the training samples improve classification accuracy. After iteration, the final changed/unchanged map and the T2 classification map are obtained.

3. Case study

3.1. Data and study area

A case study on the Landsat data was conducted to validate the effectiveness of the proposed approach. The study area is located in Xi'an city, Shaanxi province, China (34°16′N, 108°54′E). Similarly to other cities in China, the urban area of Xi'an city expanded rapidly in the last decade along with the rapid economic growth in the area. The Landsat ETM+ images acquired on 2000-06-29 and 2000-11-20 and the Landsat TM images acquired on 2010-06-17 and 2010-08-04 were used for this experiment (Fig. 3). The size of the images was 1200 × 1300 pixels, covering an area of approximately 1400 km^2. Multi-seasonal TM data were collected because these data are useful for distinguishing the cropland and forest. The forest pixels have a longer greenness period from May to October, whereas the cropland pixels have low greenness in June but approach the maximum of the growth in August. In the winter, both of the cropland and forest wilt and exhibit similar spectral characteristics. Therefore, cropland and forest pixels are particularly difficult to distinguish in the winter. CVA cannot be used in this case study because the multi-seasons in 2000 and 2010 did not correspond with each other.

A known classification map for one year is required for the proposed methodology. Here, we acquired the land cover map for 2010 (Fig. 4) from the National Geoinformatics Center of China, which was generated from TM data by visual interpretation referring to the high spatial resolution images (QuickBird). According to the land cover map, there were five land cover types in the study areas including bareland, cropland, forest, urban and water.

3.2. Updating results and accuracy assessment

The land cover map in 2000 was updated based on the multi-seasonal Landsat data and the land cover map in 2010 using the proposed method. We did not update chronologically from 2000 to 2010; instead, updated in the reverse order because the known land cover map was available in 2010. The change detection methods PCC and CVAPS were both tested for comparison. As shown in Fig. 5, the results derived from these methods based on PCC and CVAPS were very similar and exhibited a very high agreement of 97%. From 2000 to 2010, the most obvious change was urban expansion by encroaching areas with other land cover types correspondingly.

For quantitative accuracy assessment, 6398 pixels in the 2000 image were randomly selected for validation. These pixels were interpreted visually based on the experience of the authors and reference data from 2000. The accuracies of "change/unchanged" were examined first because change detection is an important part of this methodology. As shown in Tables 1 and 2, the methods based on CVAPS and PCC produced similar results, whereas PCC estimated slightly more changed areas than the CVAPS results, which is consistent with the results of a previous study (Chen et al., 2011). For classification accuracy, the confusion matrixes are shown in Tables 3 and 4. The accuracies of the two methods are also similar, while the method based on CVAPS performs slightly better. The structures of the two confused matrices are also similar. In detail, the water has the highest classification accuracy because the water spectrum is stable and unique, whereas there were much misclassification between forest and cropland, and between urban and bareland because of similar spectra. Additionally, there was also misclassification between urban and forest because trees usually cover the small towns, which results in a strong spectral vegetation signal in some urban pixels.

3.3. Role of iterated training sample selecting procedure

As a key component of the proposed methodology, the effect of the iterated training sample selecting procedure was investigated. Fig. 6a shows the relationship between the iteration number and consistence rate. The iteration ended when the consistence rate reached 99%. Both approaches that were based on CVAPS and PCC converged rapidly at the fifth and fourth iterations, respectively. This result indicates that the proposed approach does not significantly increase the computational cost.

As shown in Fig. 6b and c, the iteration largely improved the change detection and classification accuracies by more than 5% for Overall Accuracy (OA) and 0.1 for kappa. These results indicate that the proposed iterated training sample selecting process can refine the training sample and improve the change detection and classification accuracy.

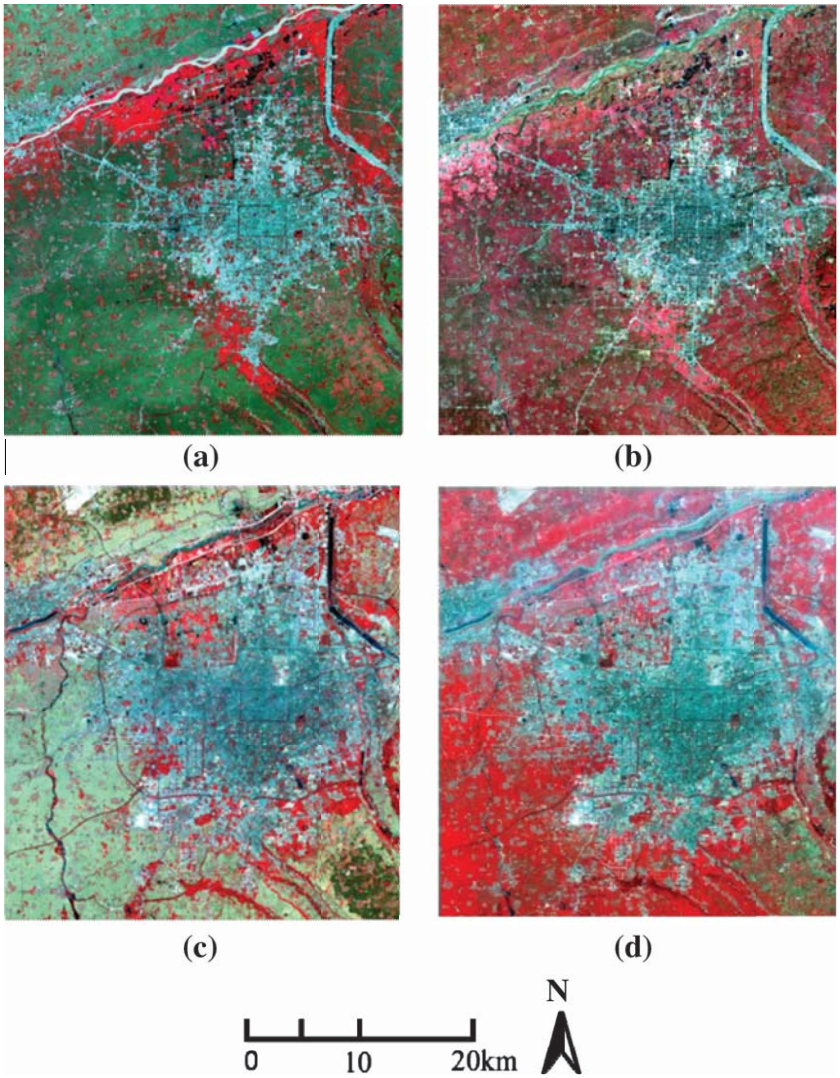

Fig. 3. Landsat TM/ETM+ images of the study area (a) ETM+ on 2000-06-29; (b) ETM+ on 2000-11-20; (c) TM on 2010-06-17; (d) TM on 2010-08-04).

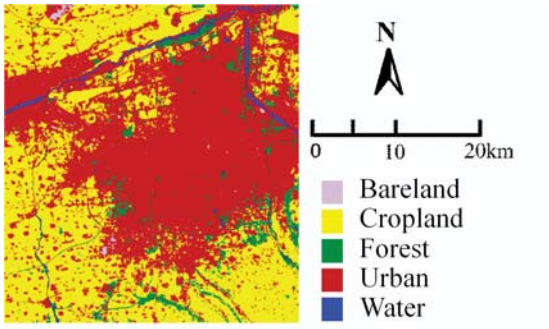

Fig. 4. Land cover map in 2010.

3.4. Role of MRF model

The methods with and without the MRF model were compared. Fig. 7 shows the updated land cover maps produced by the CVAPS-based approaches with and without the MRF model. As shown in Fig. 7, the approach with the MRF model produced more aggregated results, and the "salt-and-pepper" error was reduced significantly. The results of the PCC-based approaches are comparable, and the data are not shown in the figures. Fig. 8 compares the quantitative classification accuracies of the approaches with and without the MRF model. The MRF model improved the overall classification accuracy by approximately 5% and the kappa coefficient by approximately 0.07. The approaches based on CVAPS and PCC produced almost the same results. A limitation of the MRF model is that some thin linear objects may be removed. As shown in Fig. 9, one traffic road disappeared as the result of using the method with the MRF model. However, we still suggest using the MRF model because the classification accuracy can be improved significantly.

3.5. Role of multi-seasonal data

Compared to CVA–DTC, the proposed approach is more suitable to multi-seasonal data. Therefore, we investigated whether multi-seasonal data can improve the classification accuracy compared with single-seasonal data. Here, four single-seasonal data combinations were tested, including the images acquired on 2000-06-29 and 2010-06-17; 2000-06-29 and 2010-08-04; 2000-11-20 and 2010-06-17; and 2000-11-20 and 2010-08-04. The accuracies are compared in Fig. 10. The results derived from the multi-seasonal data achieved the highest accuracy. This is reasonable because multi-seasonal data contains phenological information, which is very useful for distinguishing the cropland and forest. In cases of single-seasonal

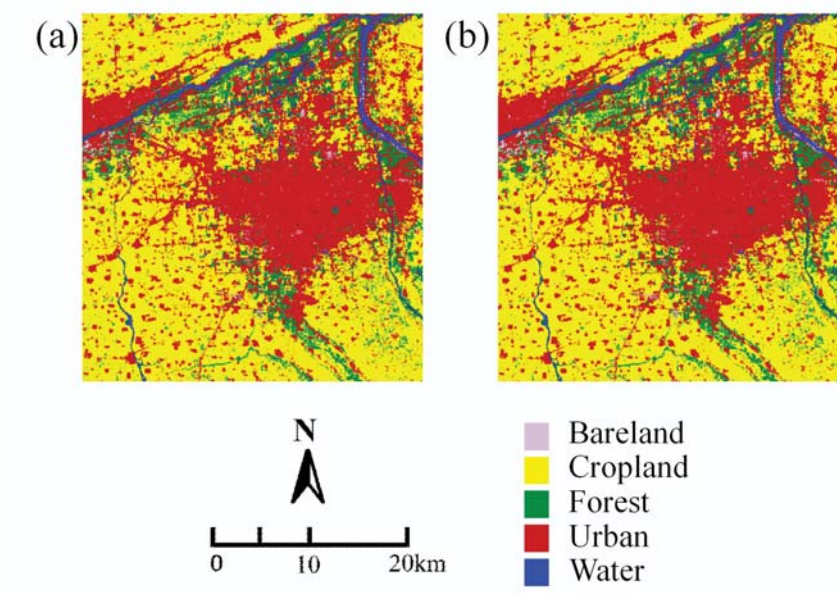

Fig. 5. Land cover map in 2000 updated by the approach based on CVAPS (a) and by the approach based on PCC (b).

Table 1
"Changed/unchanged" confusion matrix of the approach based on CVAPS.

Number of pixels	Reference changed			
	Unchanged pixels	Changed pixels	Sum	Commission error (%)
Classified changed				
Unchanged pixels	4002	600	4602	13.0
Changed pixels	230	1557	1787	12.9
Sum	4232	2157	6389	
Omission error (%)	5.43	27.8		

Overall accuracy 87.01%, kappa coefficient 0.697.

Table 2
"Changed/unchanged" confusion matrix of the approach based on PCC.

Number of pixels	Reference changed			
	Unchanged pixels	Changed pixels	Sum	Commission error (%)
Classified changed				
Unchanged pixels	3927	567	4494	12.6
Changed pixels	305	1590	1895	16.1
Sum	4232	2157	6389	
Omission error (%)	7.2	26.3		

Overall accuracy 86.3%, kappa coefficient 0.686.

data, the accuracy decreased to varying extents. In particular, the accuracy decreased largely (approximately 10% of overall accuracy and 0.10 of kappa) when TM data acquired in the winter (2000-11-20) was used. This is because cropland is very easily misclassified with deciduous forest in the winter. In most cases, the method based on CVAPS performed better than the method based on PCC. Therefore, we suggest using CVAPS in application studies.

4. Discussion and conclusion

The proposed approach uses a similar CVA–DTC strategy as Xian et al. (2009), which updated the classification map only for the changed areas. In this study, CVA was replaced with more applicable change detection techniques, CVAPS or PCC, and replaced DTC with MLC to widen the scope of its flexibility. An iterative training sample selection procedure was proposed by appropriately utilizing the unchanged area between two years to address the challenge of selecting the proper training samples without supervision. The experimental result shows that this iterative procedure can improve

Table 3
Classification confusion matrix of the approach based on CVAPS.

Number of pixels	Reference						
	Bareland	Cropland	Forest	Urban	Water	Sum	Commission error (%)
Classification							
Bareland	325	10	40	24	1	400	18.8
Cropland	7	1899	190	105	1	2202	13.8
Forest	0	187	958	0	13	1158	17.3
Urban	92	69	124	1834	39	2158	15.0
Water	9	1	13	1	456	480	5.0
Sum	433	2166	1325	1964	510	6398	
Omission error (%)	24.9	12.3	27.7	6.6	10.6		

Overall accuracy 85.5%, kappa coefficient 0.802.

Table 4
Classification confusion matrix of the approach based on PCC.

Number of pixels	Reference						
	Bareland	Cropland	Forest	Urban	Water	Sum	Commission error (%)
Classification							
Bareland	328	10	43	21	1	403	18.6
Cropland	7	1841	177	104	1	2130	13.6
Forest	0	204	967	0	15	1186	18.5
Urban	89	110	124	1838	42	2203	16.6
Water	9	1	14	1	451	476	5.3
Sum	433	2166	1325	1964	510	6398	
Omission error (%)	24.2	15.0	27.0	6.4	11.6		

Overall accuracy 84.8%, kappa coefficient 0.793.

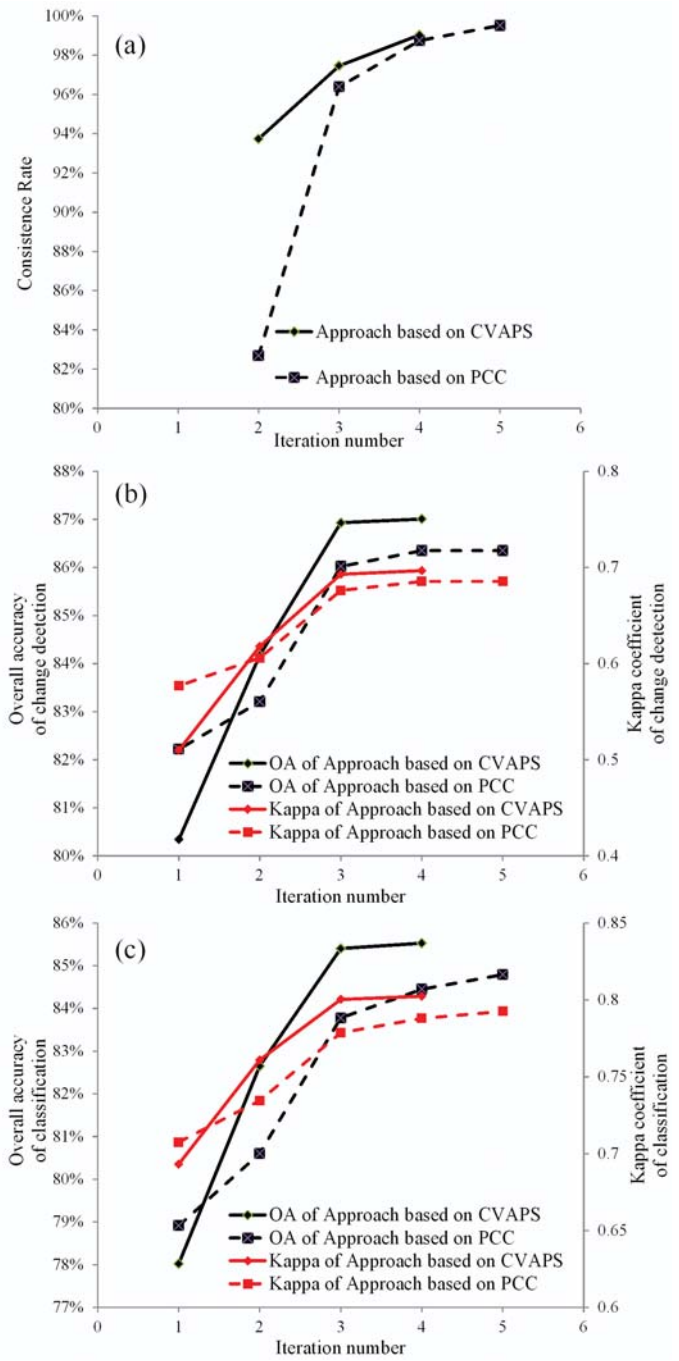

Fig. 6. Relationship between iteration number and consistence rate (a), accuracy of change detection (b), and accuracy of classification (c).

classification accuracy by approximately 5%. Furthermore, the iterative process converges in no more than five iterations, suggesting a low computational cost.

In comparison to CVA–DTC, the proposed approach employed CVAPS or PCC to detect changed areas instead of directly comparing the radiometric difference between different acquisition dates. Therefore, this method can avoid the strict requirement of CVA for reliable image radiometric correction and remotely sensed data acquisition that the two images acquired in different years should be from the same phenological period. Without such strict requirements, the proposed approach can be applied for land cover mapping or updating over larger scales and for longer periods. Additionally, the change magnitudes of different change types in CVAPS are on the same scale because the posterior probability for each pixel classification is in the range of zero to one. Consequently, a single threshold is more suitable for CVAPS than CVA, which is convenient for users to optimize the threshold with the existing thresholding methods. Compared with PCC, CVAPS analyzes the posterior probability vector with CVA, which can alleviate classification error accumulation effectively existing in PCC and improve the changed/unchanged detection accuracy. As shown in Section 3.5, CVAPS performs better than PCC in most cases. Therefore, CVAPS is recommended in applications.

In this study, MLC was employed as the supervised classification method. This method is popular and easily conducted but requires training data. In this study, an iterative training sample selecting procedure was proposed to address the limitation by appropriately utilizing the unchanged area between two years. The first step in the procedure is to use the entire known land cover map as the training data, which provides huge training samples. In the subsequent steps, the change detection result is used to refine the training samples and ensure that only unchanged pixels are used as the training reference. Regardless of the number of times the iteration is performed, the size of training samples for classification is still very large, which is nearly equal to the size of the unchanged area. MLC is more suitable for such large training samples because the huge size of training samples is more likely to satisfy the normal distribution assumed in MLC. The advantage of the non-parameter classification algorithms, such as SVM and ANN, is the low requirement for specific spectral distribution. Another advantage of SVM is its robustness for the small training sample size. These advantages are not shown obviously in the case of a large sample size. Instead, the computation cost increases geometrically with the increase in training sample size. Therefore, the non-parameter algorithms are not considered in this approach. However, any supervised classifiers can be used in our approach in theory. In the future, more advanced classifiers can be employed.

MRF model is also an important sub-module in this approach. The experiment result shows that it can reduce "salt and pepper" error significantly although some thin linear objects may also be removed mistakenly. In this study, a standard MRF model was employed for general feasibility. However, if some prior knowledge, for example the land cover incompatible/compatible rules among spatial or temporal neighborhood pixels, are available(Liu et al., 2006, 2008), they also can be integrated into the MRF model to meet the specific need of a study.

In practice, updating a land cover map often depends on data availability and quality, time and cost constraints, and analytical skill and experience. Compared with CVA–DTC and T-SFE, the proposed approach requires no supervision and decreased requirements for remotely sensed data, which is applicable to timely updates of both historical and future land cover maps.

We also recognize that there are potential limitations regarding this new approach. Firstly, this approach assumes the same classification systems between two years. Therefore, the new land cover type will not be correctly identified if it is not available on T1 but appears on T2. In this case, the new land cover type on T2 should be firstly identified before using the proposed approach. One-class classifier (e.g. Muñoz-Marí et al., 2010) may be a good choice for identifying the new land cover type because only the training sample of the new class is required. Another limitation is that the approach does require the availability of one reliable land cover map that provides initial training samples. In general, a high quality classified map is expected. When the amount of misclassification pixels accounts only for a small proportion, the estimation of mean value and covariance of each class in MLC will be affected very slightly; consequently, the posterior probability calculated from MLC will also be affected slightly. However, if the classification accuracy of the known land cover map is poor, the accuracy of both

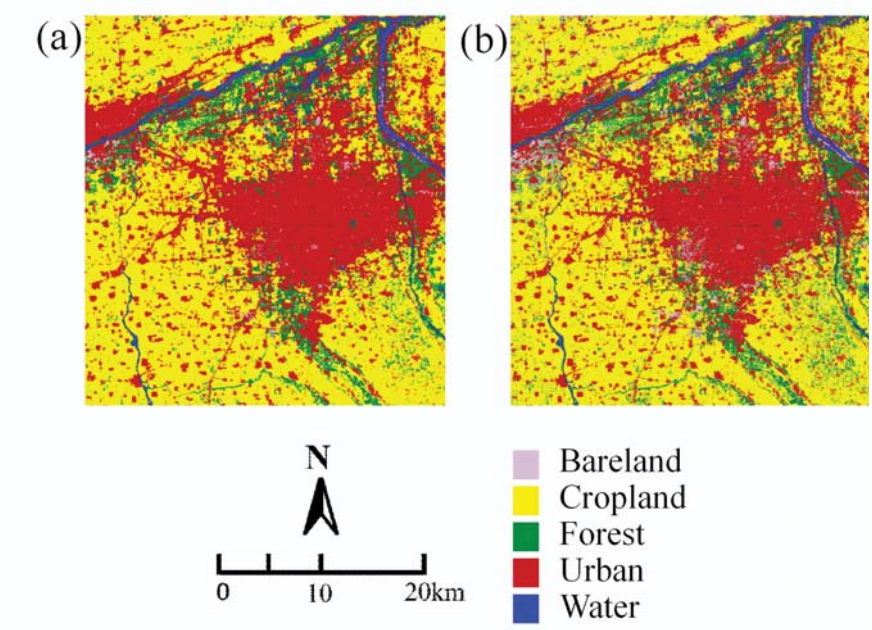

Fig. 7. Land cover map in 2000 updated by the approach of CVAPS with MRF model (a) and without MRF model (b).

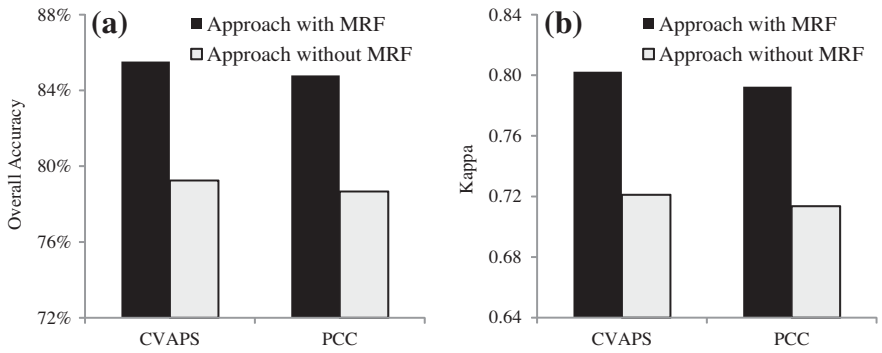

Fig. 8. Comparison of the classification accuracies of the proposed approaches with and without the MRF model (a) overall accuracy; (b) kappa coefficient.

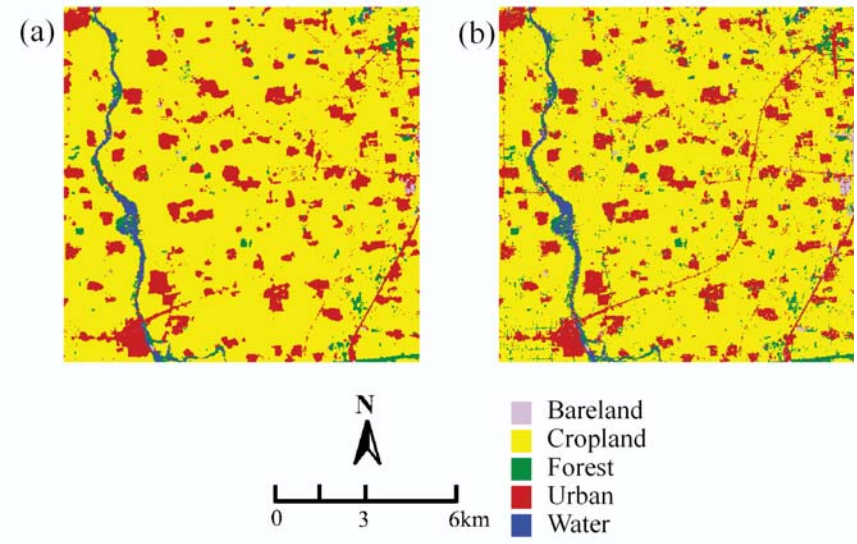

Fig. 9. Detailed comparison of the approaches with and without the MRF model (a) with MRF model and (b) without MRF model.

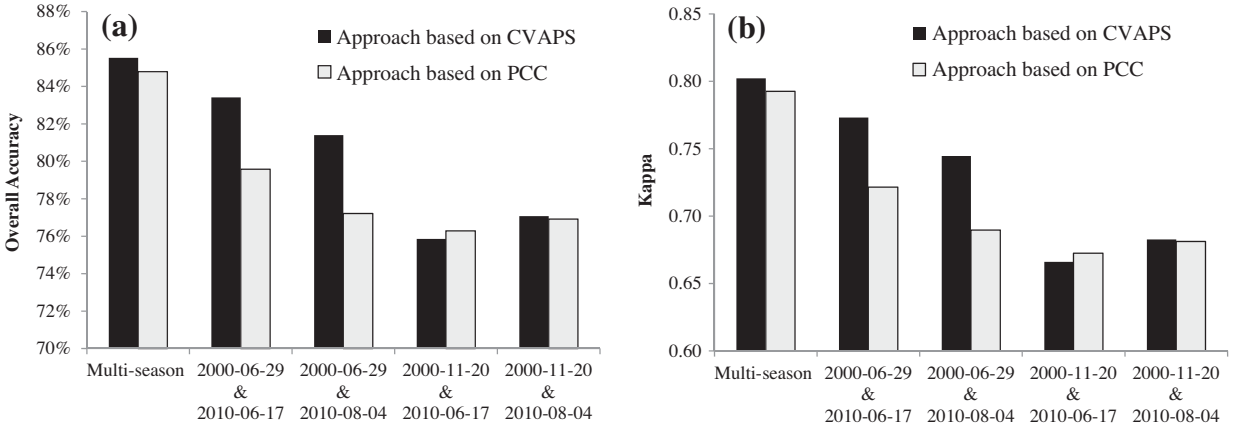

Fig. 10. Accuracies of classification results based on multi-seasonal and single-seasonal data (a) overall accuracy; (b) kappa coefficient.

change detection and classification may be reduced. The impact of error propagation could be complicated, depending on the spectral and spatial distribution of the misclassification pixels. Some possible solutions include selecting core areas of different land cover types in the known map as a training reference instead of using the entire map in the first step or manually selecting the areas with lower classification uncertainty if such information is available.

Acknowledgements

This study was partially funded by the 863 project of China (2009AA122004) and the International S&T Cooperation Program (2010DFB10030).

References

Aitkenhead, M.J., Aalders, I.H., 2011. Automating land cover mapping of Scotland using expert system and knowledge integration methods. Remote Sensing of Environment 115 (5), 1285–1295.

Arino, O., Bicheron, P., Achard, F., Latham, J., Witt, R., Weber, J.L., 2008. GLOBCOVER: the most detailed portrait of the earth. ESA Bulletin – European Space Agency 136, 24–31.

Bartholomé, E., Belward, A.S., 2005. GLC2000: a new approach to global land cover mapping from Earth Observation data. International Journal of Remote Sensing 26 (9), 1959–1977.

Besag, J., 1986. On the statistical analysis of dirty pictures. Journal of Royal Statistical Society, Series B (Methodological) 48 (3), 259–302.

Blaschke, T., 2010. Object based image analysis for remote sensing. ISPRS Journal of Photogrammetry and Remote Sensing 65 (1), 2–16.

Bruzzone, L., Prieto, D.F., 2000. Automatic analysis of the difference image for unsupervised change detection. IEEE Transactions on Geoscience and Remote Sensing 38 (3), 1171–1182.

Canty, M.J., 2006. Image Analysis, Classification and Change Detection in remote Sensing with Algorithms for ENVI/IDL. Taylor & Francis, CRC Press.

Castellana, L., D'Addabbo, A., Pasquariello, 2007. A composed supervised/unsupervised approach to improve change detection from remote sensing. Pattern Recognition Letters 28 (4), 405–413.

Chen, J., Gong, P., He, C., Pu, R., Shi, P., 2003. Land-use/land-cover change detection using improved change-vector analysis. Photogrammetric Engineering & Remote Sensing 69 (4), 369–379.

Chen, J., Chen, X., Cui, X., Chen, J., 2011. Change vector analysis in posterior probability space: a new method for land cover change detection. IEEE Geoscience and Remote Sensing Letters 8 (2), 317–321.

Dixon, B., Candade, N., 2007. Multispectral land use classification using neural networks and support vector machine: one or the other, or both? International Journal of Remote Sensing 29 (4), 1185–1206.

Franklin, S.E., Wulder, M.A., 2002. Remote sensing methods in medium spatial resolution satellite data land cover classification of large areas. Progress in Physical Geography 26 (2), 173–205.

Friedl, M.A., McIver, D.K., Hodges, J.C.F., Zhang, X.Y., Muchoney, D., Strahler, A.H., Woodcock, C.E., Gopal, S., Schneider, A., Cooper, A., Baccini, A., Gao, F., Schaaf, C., 2002. Global land cover mapping from MODIS: algorithms and early results. Remote Sensing of Environment 83 (1–2), 287–302.

Hansen, M.C., Reed, B., 2000. A comparison of the IGBP DISCover and University of Maryland 1 km global land cover products. International Journal of Remote Sensing 21 (6–7), 1365–1373.

Hansen, M.C., Defries, R.S., Townshend, J.R.G., Sohlberg, R., 2000. Global land cover classification at 1 km spatial resolution using a classification forest approach. International Journal of Remote Sensing 21 (6–7), 1331–1364.

Ho, L.T.K., Umitsu, M., 2011. Micro-landform classification and flood hazard assessment of the Thu Bon alluvial plain, central Vietnam via an integrated method utilizing remotely sensed data. Applied Geography 31 (3), 1082–1093.

Iwao, K., Nishida, K., Kinoshita, T., Yamagata, Y., 2006. Validating land cover maps with degree confluence project information. Geophysical Research Letters 33, L23404.

Jeon, B., Landgrebe, D.A., 1991. Spatio-temporal contextual classification based on Markov random field model. In: Proceedings of the International Geoscience and Remote Sensing Symposium (IGARSS), June, pp. 1819–1822.

Kaptué Tchuenté, A.T., Roujean, J.L., de Jong, S.M., 2011. Comparison and relative quality assessment of the GLC2000, GLOBCOVER, MODIS and ECOCLIMAP land cover data sets at the African continental scale. International Journal of Applied Earth Observation and Geoinformation 13 (2), 207–219.

Kapur, J.N., Sahoo, P.K., Wong, A.K.C., 1985. A new method for gray level picture thresholding using the entropy of the histogram. Computer Vision, Graphics, and Image Processing 29 (3), 273–285.

Kohli, P., Torr, P.H.S., 2007. Dynamic graph cuts for efficient inference in Markov Random Fields. IEEE Transactions on Pattern Analysis and Machine Intelligence 29 (12), 2079–2088.

Liu, D., Maggi, K., Gong, P., 2006. A spatial–temporal approach to monitoring forest disease spread using multi-temporal high spatial resolution imagery. Remote Sensing of Environment 101 (2), 167–180.

Liu, D., Song, K., Townshend, J.R.G., Gong, P., 2008. Using local transition probability models in Markov random fields for forest change detection. Remote Sensing of Environment 112 (5), 2222–2231.

Loveland, T.R., Reed, B.C., Brown, J.F., Ohlen, D.O., Zhu, Z., Yang, L., Merchant, J.W., 2000. Development of a global land cover characteristics database and IGBP DISCover from 1 km AVHRR data. International Journal of Remote Sensing 21 (6–7), 1303–1330.

Lu, D., Weng, Q., 2007. A survey of image classification methods and techniques for improving classification performance. International Journal of Remote Sensing 28 (5), 823–870.

Lu, D., Mausel, P., Brondizio, E., Moran, E., 2004. Change detection techniques. International Journal of Remote Sensing 25 (12), 2365–2407.

Macleod, D.R., Congalton, G.R., 1998. A quantitative comparison of change detection algorithms for monitoring eelgrass from remotely sensed data. Photogrammetric Engineering & Remote Sensing 64 (3), 207–216.

Maxwell, S.K., Nuckols, J.R., Ward, M.H., Hoffer, R.M., 2004. An automatic approach to mapping corn from Landsat imagery. Computers and Electronics in Agriculture 43 (1), 43–54.

Mountrakis, G., Im, J., Ogole, C., 2011. Support vector machines in remote sensing: a review. ISPRS Journal of Photogrammetry and Remote Sensing 66 (3), 247–259.

Muñoz-Marí, J., Bovolo, F., Gómez-Chova, L., Bruzzone, L., Camps-Valls, G., 2010. Semisupervised one-class support vector machines for classification of remote sensing data. IEEE Transactions on Geoscience and Remote Sensing 48 (8), 3188–3197.

Negi, H.S., Kulkarni, A.V., Semwal, B.S., 2009. Estimation of snow cover distribution in Beas basin, Indian Himalaya using satellite data and ground measurements. Journal of Earth System Science 118 (5), 525–538.

Saadat, H., Adamowski, J., Bonnell, R., Sharifi, F., Namdar, M., 2011. Land use and land cover classification over a large area in Iran based on single date analysis of satellite imagery. ISPRS Journal of Photogrammetry and Remote Sensing 66 (5), 608–619.

Serra, P., Pons, X., Sauru, D., 2003. Post-classification change detection with data from different sensors: some accuracy consideration. International Journal of Remote Sensing 24 (16), 3311–3340.

Solberg, A.H.S., Taxt, T., Jain, A.K., 1996. A markov random field model for classification of multisource satellite imagery. IEEE Transactions on Geoscience and Remote Sensing 34 (1), 100–113.

Sui, H., Peng, F., Xu, C., Sun, K., Gong, J., 2012. GPU-accelerated MRF segmentation algorithm for SAR images. Computer and Geosciences 43, 159–166.
Szeliski, R., Zabih, R., Scharstein, D., Veksler, O., Kolmogorov, V., Agarwala, A., Tappen, M., Rother, C., 2008. A comparative study of energy minimization methods for Markov random fields with smoothness-based priors. IEEE Transactions on Pattern Analysis and Machine Intelligence 30 (6), 1068–1080.
Turner, B.L., Skole, D., Sanderson, S., Fischer, G., Fresco, L., Leemans, R., 1995, Land-use and Land-cover Change Science/Research Plan, IGBP Report No. 35.
Weng, Q., 2011. Advances in Environmental Remote Sensing: Sensors, Algorithms and Applications. CRC Press/Taylor and Francis, Boca Raton, FL, USA.
Xian, G., Collin, H., Fry, J., 2009. Updating the 2001 National Land Cover Database land cover classification to 2006 by using Landsat imagery change detection methods. Remote Sensing of Environment 113 (6), 1133–1147.
Xie, Y., Sha, Z., Bai, Y., 2010. Classifying historical remotely sensed imagery using a tempo-spatial feature evolution (T-SFE) model. ISPRS Journal of Photogrammetry and Remote Sensing 65 (2), 182–190.